Research Article

Evaluating the Mechanical and Tribological Properties of DLC Nanocoated Aluminium 5051 Using RF Sputtering

L. Natrayan [ID],[1] **Anjibabu Merneedi** [ID],[2] **Dhinakaran Veeman** [ID],[3] **S. Kaliappan** [ID],[4] **P. Satyanarayana Raju,**[5] **Ram Subbiah,**[6] **and S. Venkatesh Kumar** [ID][7]

[1]Department of Mechanical Engineering, Saveetha School of Engineering, SIMATS, Chennai, Tamil Nadu 602105, India
[2]Department of Mechanical Engineering, Aditya College of Engineering, Surampalem, 533437 Andhra Pradesh, India
[3]Centre for Additive Manufacturing, Chennai Institute of Technology, 600069, Chennai, India
[4]Department of Mechanical Engineering, Velammal Institute of Technology, Chennai, 601204 Tamil Nadu, India
[5]Department of Mechanical Engineering, Vardhaman College of Engineering, Kacharam, Shamshabad, Hyderabad, 501218 Telangana, India
[6]Department of Mechanical Engineering, Gokaraju Rangaraju Institute of Engineering and Technology, Hyderabad, India
[7]Department of Mechanical Engineering, College of Engineering and Technology, Mettu University, Ethiopia P.O. Box: 318

Correspondence should be addressed to L. Natrayan; natrayanphd@gmail.com
and S. Venkatesh Kumar; s.venkateshkumar@meu.edu.et

The diamond-like carbon- (DLC-) coating technique is used in the sliding parts of automotive engines, among other applications, to reduce friction and wear. In this work, DLC has been coated on the Aluminium 5051 sample to assess the mechanical and tribological properties. A sputtering deposition mechanism is used, and the DLC is coated using a graphite target. The developed DLC coatings are tested for adhesion strength, hardness, chemical composition using XRD, and wear behaviour. The developed DLC thin films have considerably increased the wear behaviour of the Aluminium 5051 sample and have fulfilled the objective of this study. The XRD data indicated the presence of amorphous carbon in the coating with a threefold increase to the hardness of the naked aluminium. This study provides insight into improving the aluminium wear resistance by developing a considerably hard coating.

1. Introduction

In today's machinery sector, surface engineering is critical. Hard coatings extend the service life of tools and moulds, yet hard coatings are difficult to apply to machine parts built of soft materials such as aluminium [1]. Thin films with high hardness can bear higher loads, but as the substrate is a soft material, the substrate fails the coating and the thin film too shall fail [2]. Surfaces take up a very little area in a matter when compared to the bulk. Still, they are extremely difficult to investigate [3] due to the very asymmetric nature of the forces acting on the surfaces. Pristine surfaces are highly susceptible to impurities and flaws. When two extremely pure surfaces come into contact, adhesive force is created, and

energy is used to separate those surfaces [4]. Adhesion energy is the energy exerted by atoms on the outer surfaces of nearby atoms when they come into contact with each other [5]. A simple van der Waal, covalent, ionic, or electrostatic force can be used as adhesive forces [6]. Cohesive forces hold atoms together in bulk materials. Atoms are held together by a cohesive force, and it takes a lot of force to rip a substance in half [7]. The breaking of cohesive links between atoms causes the metal to tear. The atoms with broken cohesive bonds on the new surfaces generated after breaking the parent material will be readily attracted to the new atoms [8]. Surface energy is the excess free energy per unit area on a crystal's surface. It is denoted by and plays a crucial role in thin-film adherence to the substrate. Surface tension

values of liquid metals can be extrapolated to absolute zero, or crystal cleavage can be used to compute this [9]. Other than the actual approaches, there are several theoretical ways to calculate surface energy. There are disparities between practical and theoretical values, and no theoretical value equates to a practical value. The presence of numerous faults and impurities in a chosen crystal is the primary source of this mismatch, and obtaining a crystal-free of defects or impurities is difficult [10]. Bazan et al. concluded that the CF-reinforced epoxy composites exhibit 14% reduction in ILSS, when the samples are aged hydrothermally at 60°C and at 95% humidity for 1200 hours, and this is due to the crack initiation at the interface which is caused by thermal stress [11]. Shrivastava and Singh concluded that the UD and BD CF-reinforced epoxy composites exhibit 20% and 75% increase in flexural strength, respectively, due to the growth of CNTs on the surface thereby resulting in good adhesion with the matrix [12]. An et al. found that the CF-reinforced epoxy composites with CNTs grown by an aerosol-assisted CVD process exhibit 94% increase in IFSS and 210% increase in surface area because of the formation of the 3D structure on the surface of the fiber, and also, the fiber diameter is increased from 7 micrometres to 20 micrometres [13].

In general, adhesion can be attributed to the sticking of two surfaces with each other. Technically, adhesion is defined as the transfer of mechanical energy in shear between two surfaces without any damage to the surfaces or the interface by a slip or inelastic displacement [14]. The most difficult aspect of thin-film adhesion is determining the strength of the adhesion between the thin film and the substrate. Even though numerous approaches have been created, it is critical to select the appropriate process based on the nature of the coating, substrate, and type of bonding between the two [15]. There is a wealth of information for thin-film adhesion on the many types and adhesion measurement methods. Simple pull tests, scratch tests, X-ray spectroscopy, nanoindentation scratch, and laser spallation are among the methods used. According to Tamtögl et al., theoretical approaches measure theoretical forces at the atomic level [16]. The observations include the nucleation rate, island density measurement, critical condensation, and residence time of depositing atoms. Adhesion between substrate and coating can be viewed on an atomic scale as adsorption energy between substrate surface atoms and coating atoms. Breaking the links between these atoms suffices to remove the coating from the substrate [17]. So, by measuring the total adsorption energy between atoms and relating it to all atoms, these approaches measure the total adsorption energy present between atoms to break the bond. A smooth round stylus is drawn on a hard-coated sample in a scratch test by gradually increasing the load. When the coating breaks and peels away from the substrate, the stylus is halted and the critical load recorded [18]. Even though it appears like a simple compression force applied by the stylus and the substrate is separating the coating, many complex forces are at work in this test. The load causes plastic deformation of the substrate, while the stylus penetrates the coating and causes shear strain. This process increases ther-

momechanical reactions with the viscoelastic flow, interfacial failure, and bulk fracture [19]. Scratch tests are difficult to test to study as a result of this. A direct tensile force is imparted to the film by pulling it off the substrate with a pin or rod attached in the usual direction. This approach can be used to attach thin films, as well as other sticky surfaces and objects. The failure that occurs at the substrate-thin-film contact is referred to as adhesion force [20].

Butler invented the toppling test by modifying the direct pulling method. Instead of using the conventional force, he used a brass rod with two legs to impart force laterally to the thin sheet. When a load is applied, one leg applies compressive force while the other exerts tensile force, causing the film to peel. Karapappas et al. observed that the CF-reinforced epoxy composites incorporated with 0.1% CNT exhibit reduced mechanical properties and 1% incorporation of CNT leads to enhancement of fracture energy by 45 to 75% [21]. Konuru et al. reported that the CF-reinforced epoxy composites exhibit incremental IFSS by 70 to 200%, depending on CNT deposition time on the CF surface [22]. Yogeshwaran et al. found that the CF-reinforced epoxy composites with CNTs grown on the surface possess 150 to 300% increased toughness due to different aspect ratios of the CNT [23]. Surface modification of many metals is done with DLC (diamond-like carbon) thin film. These thin films have good wear resistance along with corrosion resistance and hardness. DLC films are amorphous carbon materials containing sp^3 and sp^2 bonds that are metastable. DLC films have received much attention among all surface treatment materials because of their exceptional tribological properties. The DLC film is increasingly being used as a protective layer. It is associated with the percentage of sp3 bonds in the films, and for example, it has a low coefficient of friction and good wear resistance. On the other hand, it is critical to reducing the friction and wear of the inner wall surface of many industrial components with undetectable holes, such as dies, bushings, and pipes, as a type of industrial application. DLC has high mechanical properties like high wear resistance and low friction, which are highly desirable for industrial applications. DLC nanocoated Aluminium 5051 is mainly used to reduce the sliding friction of moving parts.

Novel in the research work is that DLC has been coated on the Aluminium 5051 sample to assess the mechanical and tribological properties. A sputtering deposition mechanism technique is used in this research work. The developed DLC coatings were tested for adhesion strength, hardness, chemical composition using XRD, and wear behaviour.

2. Methodology

The RF sputtering procedure was used to place graphite targets on aluminium. Graphite targets with a purity of 99.99%, a diameter of 50 mm, and a thickness of 3.0 mm were procured from Testbourne and utilized for the current study. Figure 1 depicts a schematic design of the experimental system. The magnetron on which the target material to be coated is placed is connected to the RF power supply through an impedance matching network. The magnetron serves as an electrode, and the entire chamber is grounded.
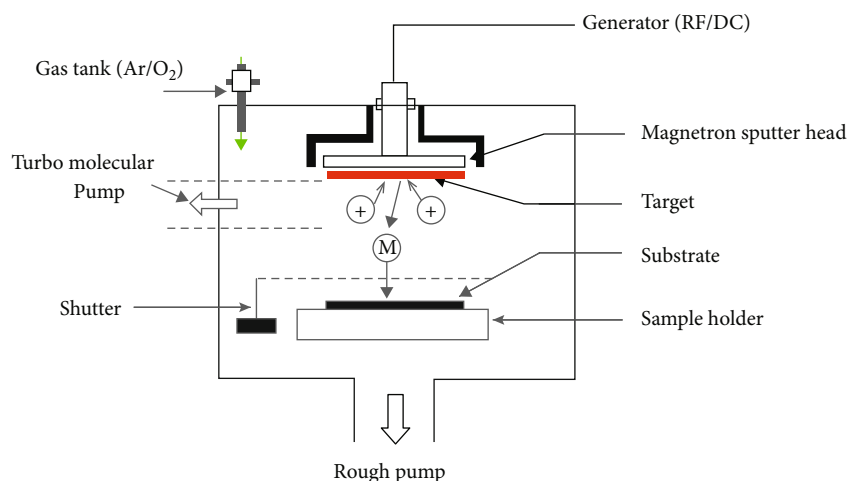
FIGURE 1: Schematic representation of sputtering machine.

FIGURE 2: Aluminium 5051 plate ($10 \times 20 \times 3$ mm).

TABLE 1: Measured hardness values of samples deposited at room temperature along with modulus values.

Sample	100 W	200 W	300 W	400 W
Hardness (GPa)	10.6	13.5	18.2	12.3
Modulus (GPa)	51.3	70.2	120	68.1

TABLE 2: Measured hardness values of samples deposited at 500 degrees along with modulus values.

Sample	100 W	200 W	300 W	400 W
Hardness (GPa)	15.1	20.8	22.5	20.1
Modulus (GPa)	76.2	111.2	130.5	100.6

In this experiment, the sputtering power was changed in stages of 100 W from 100 to 400 W.

Aluminium is cut into $10 \times 20 \times 3$ mm substrates and ground to a high level of precision of order 0.5 m using various grades of abrasive papers and diamond polish. Aluminium 5051 plates are shown in Figure 2. With acetone solution, aluminium samples are cleaned and etched in Ar plasma for 10 minutes before sputtering. Working pressure is maintained at 10^{-2} bar in the vacuum chamber and used for the turbopump. The temperature of the substrate is monitored and can be adjusted manually by the substrate holder. For the temperature-dependent adhesion qualities, two different substrate temperatures were used: room temperature and 500 degrees. A total thickness of the film 1200 nm is achieved for the DLC thin films.

The nanoindentation procedure is used to measure the hardness and elastic modulus. At a specified temperature and working pressure, samples are mounted on resin for stabilization. The nanoindentation machine with model G200 from Agilent Technologies is utilized for Berkovich indenter indentations in nanoindentation operations. A scratch test is done on the samples for estimating the adhesion of the developed DLC coatings. The same machine used for nanoindentation is used for the scratch analysis with the Berkovich indenter. Load is gradually increased to identify the critical load at which the DLC coating peels off. This load is taken as the ultimate load and is considered as adhesion strength of the film.

The pin on disk is carried out to find the wear and friction of the samples; the pin is the aluminium sample without any coating, and the disk is aluminium coated with DLC. XRD analysis is done on the DLC samples to find the chemical composition of the coating. A load of 100 gm is used for the test, and a total of 500 is carried out.

3. Results and Discussion

3.1. Hardness. Tables 1 and 2 show the hardness and modulus values of the developed thin films measured by nanoindentation by the load vs. deflection method. The Berkovich indenter was used to apply a load in the micronewton range.

The hardness of the coated hard thin films is hard to measure as the soft substrate takes away all the load, so an underreported value is measured. It is difficult to detect the hardness and elastic modulus of the coating using regular indentation. The substrate effect is unavoidable in this scenario, regardless of whether the 10% thickness criterion is implemented. The soft substrate cushioned the rigid thin-film coating. The DLC coating is extremely rigid, and it directly applies the load to the substrate. When a load is applied, elastic deformation occurs on the substrate, and the hardness under the load is measured. As a result, the
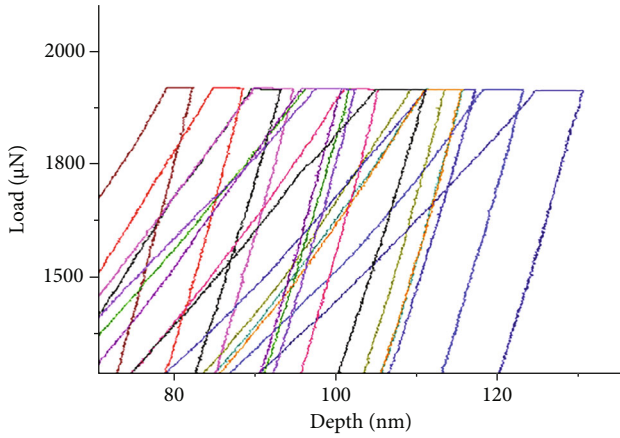
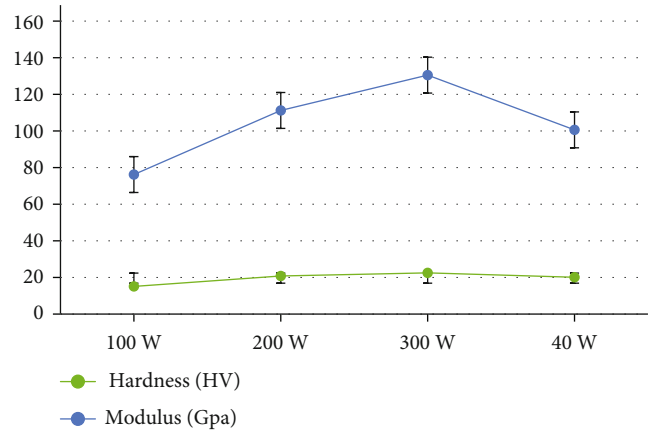FIGURE 3: Load vs. displacement curves developed by nanoindentation data.

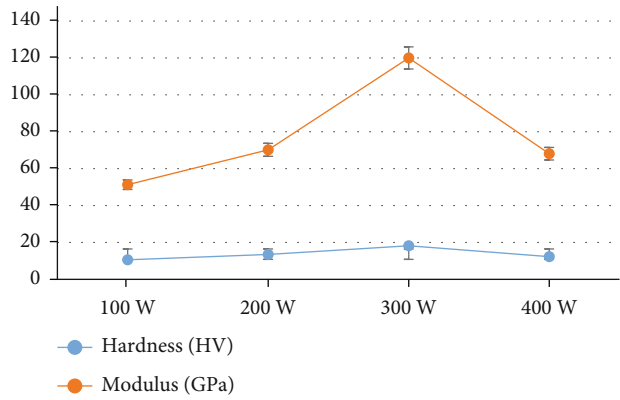FIGURE 4: Hardness and modulus values of samples deposited at room temperature.

FIGURE 5: Hardness and modulus values of samples deposited at 500 degrees.

TABLE 3: Adhesion strength of DLC films.

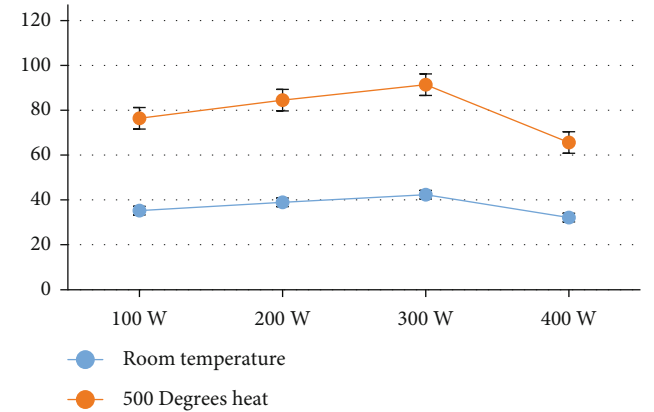| Sample	Room temperature	500-degree heat
100 W	35.2	41.2
200 W	38.9	45.6
300 W	42.3	49.1
400 W	32.1	33.5

FIGURE 6: Adhesion strength of DLC films.

FIGURE 7: XRD graph of DLC coating.

findings achieved in this situation are the coating and substrate's combined hardness, which considerably reduced the coating's ensuing qualities. On each sample, many trials were conducted, and the average hardness and modulus of elasticity were computed. The area is calculated when the load is withdrawn to identify the sample's exact hardness. At the maximum load, all trials were assigned a holding time of 15.0 seconds.

The hardness of the samples is calculated, and the highest hardness is measured for samples deposited at higher substrate temperature conditions. For the samples deposited at room temperature conditions, the hardness is less compared to other samples. As the deposition power increases from 100 W to 400 W, the hardness increases up to 300 W. It decreases for 400 W. This trend is observed for both room temperature and high-temperature deposition conditions [24]. The highest hardness increment found for the room temperature deposition condition is 71%, as the sputtering power is increased from 100 W to 300 W. In contrast, the hardness increment is 42% when the deposition power is increased from 100 W to 300 W. Figure 3 shows the load vs. displacement diagram achieved using nanoindentation data. Figures 4 and 5 represent hardness and modulus data of samples in graphical form.
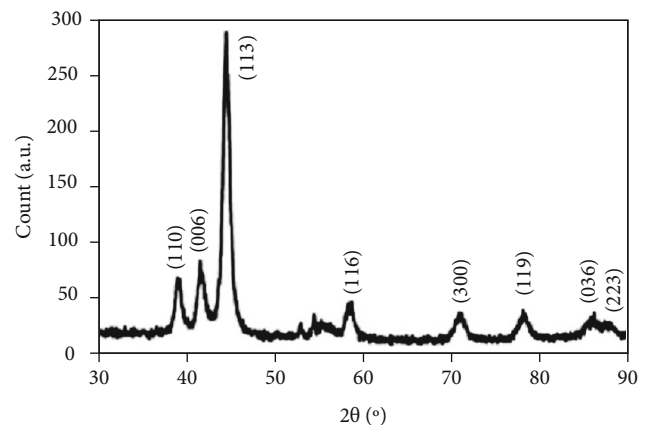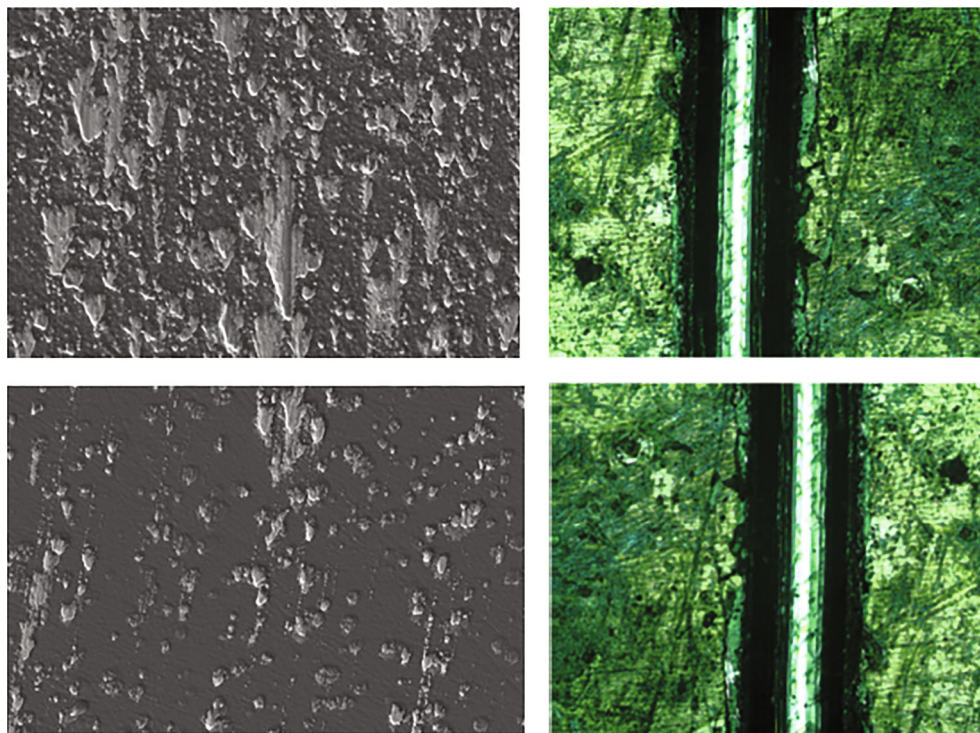
FIGURE 8: Wear track of DLC coating.

3.2. Adhesion Strength. The adhesion strength of the DLC films is measured by using a nanoscratch test. The values of the results obtained are given in Table 3. The adhesion strength of the samples increases with the increment in the substrate power up to 300 W. From 300 W to 400 W, the adhesion strength is found to decrease drastically [25]. This trend is observed for both room temperature deposited and high temperature deposited samples. The decrement in the adhesion can be attributed to the high stresses developed in the film deposition process when the sputtering power increases.

As the power increases, the depositing atoms come with higher energy and strikes the depositing material; this causes stress at the atom strike site. Before these stresses dissipate, other atoms get deposited on top of it causing stress concentration [26]. The adhesion strength is higher for the samples deposited at higher temperatures than the room temperature deposition samples. The reason for the higher adhesion is the stress-relieving phenomena taking place during the substrate heating process [27]. The substrate temperature acts as annealing during the deposition process and relieves stress, thus increasing the adhesion strength. The graphical representation of the adhesion strength is given in Figure 6.

3.3. XRD Analysis. The XRD analysis shows the presence of amorphous carbon in the DLC coating. The XRD graph is presented in Figure 7. The sample is kept in an XRD machine and swept from $20°$ to $90°$ angles for analysis [28]. There are no other peaks other than carbon, and the detected carbon is in amorphous graphite without crystalline diamond form. It indicates there are sp^2 bonds in the devel-

oped films but not sp^3, which helps in a further increase in the hardness of the film [29].

3.4. Wear Test. The coating samples were put through a dry wear test in a pin-on-disk mode with an aluminium pin as the counter body. Figure 8 shows the wear track of the DLC coating. The samples' coefficients of friction (COF) range from 0.10 to 0.15. The COF of the high temperature-DLC sample is marginally greater than the COF of the room temperature-DLC sample at the same test load [30]. The COF curves of the SNC-DLC sample have some variations. During the test, it appears that this sample suffers from abrasion wear. Despite this, the COF for both coating samples (COF0.15) is very low [31].

3.5. Raman Spectroscopy. Raman spectroscopy is a common technique for identifying diamonds, graphite, and other carbon-based materials. The Raman spectra have two large peaks for amorphous carbon: 1200–$1450\,cm^{-1}$ for the D mode and 1500–$1700\,cm^{-1}$ for the G mode. The G band is attributed to sp^2 graphite-like microdomain graphite-like layers, whereas the D band is attributed to the bond-angle disorder in the sp^2 graphite-like microdomains.

The tested sample which is used for XRD has been tested for the Raman spectroscopy. The sample showed the presence of sp^2 bonds majorly in the DLC and the traces of sp^3. The Raman spectra in Figure 9 shows two broad peaks centred around $1348\,cm^{-1}$ (D-line) and $1600\,cm^{-1}$ (G-line). The peak about $1600\,cm^{-1}$ could be noticeably different from the crystalline graphite's characteristic sharp peak around $1580\,cm^{-1}$. It demonstrates that the film is a normal DLC film with a combination of sp^2 and sp^3 carbon structures.
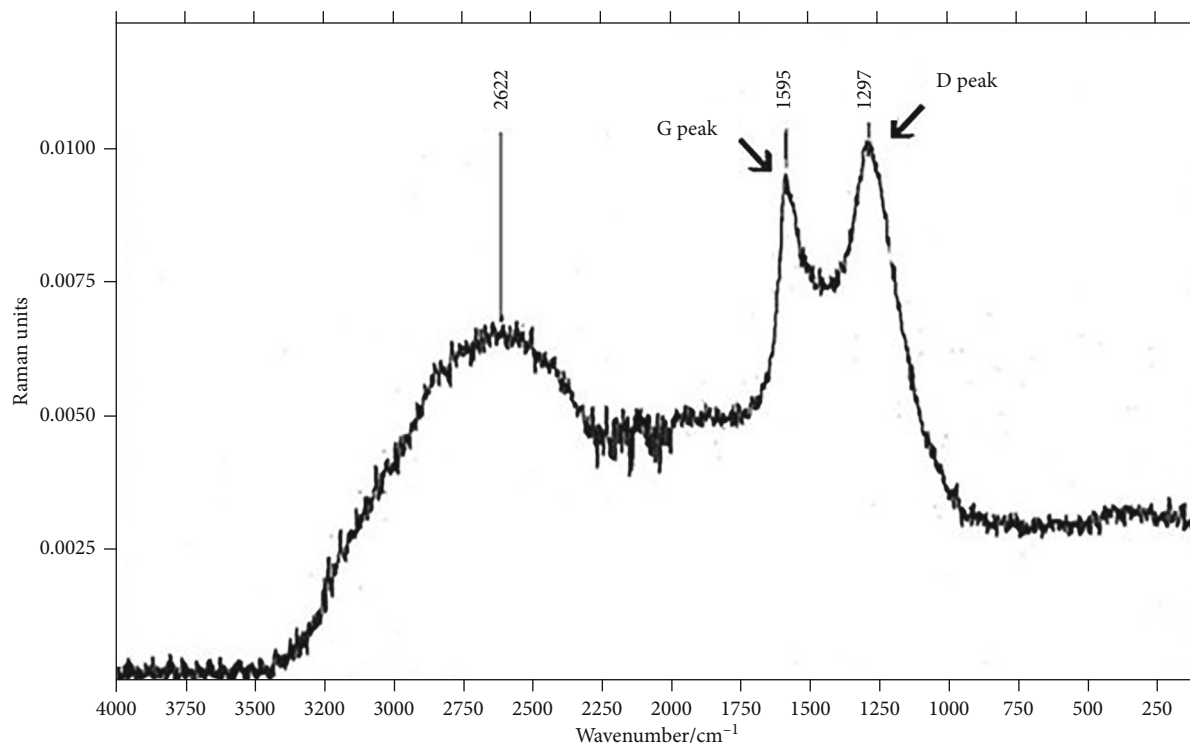
FIGURE 9: Raman spectra of DLC film.

4. Conclusion

The DLC thin films have been successfully developed on the Aluminium 5051 samples by the sputtering deposition method. The substrate heating during the deposition process plays a crucial role in the adhesion of the film and its hardness. By changing the sputtering deposition power, the films' hardness and adhesion can be tailor-made. A total hardness increment of 71% can be achieved by changing the sputtering power in the deposition. By incorporating substrate heat and 300 W power, the highest hardness can be achieved for the given aluminium DLC thin film. The adhesion is also influenced by the substrate temperature as well as power, and the highest adhesion strength can be achieved for substrate heating and 300 W power DLC thin film. XRD and Raman spectroscopy indicated the presence of amorphous graphite in the DLC films rather than the crystal diamond form and is mainly due to the formation of sp^2 bonds in the DLC rather than sp^3 bonds.

Data Availability

The data used to support the findings of this study are included in the article. Should further data or information be required, these are available from the corresponding author upon request.

Disclosure

This study was performed as a part of the Employment of the College of Engineering and Technology, Mettu University, Ethiopia.

Conflicts of Interest

The authors declare that there are no conflicts of interest regarding the publication of this paper.

Acknowledgments

References

[1] M. Aamir, K. Giasin, M. Tolouei-Rad, and A. Vafadar, "A review: drilling performance and hole quality of aluminium alloys for aerospace applications," *Journal of Materials Research and Technology*, vol. 9, no. 6, pp. 12484–12500, 2020.

[2] L. Patnaik, S. R. Maity, and S. Kumar, "Mechanical and tribological assessment of composite AlCrN or a-C:Ag-based thin films for implant application," *Ceramics International*, vol. 47, no. 5, pp. 6736–6752, 2021.

[3] L. H. Hu and Y. K. Wang, "Silicon carbonitride ceramic surface-modified nanoporous aluminum alloy by preceramic polysilazane precursor for surface strengthening," *Materials Science and Engineering: B*, vol. 267, article 115113, 2021.

[4] I. Suresh Kannan and A. Ghosh, "Anti-friction and wetting behavior of a new polymer composite coating towards aluminium and dry machining of AA2024 alloy by coated end mills," *Journal of Materials Processing Technology*, vol. 252, pp. 280–293, 2018.

[5] G. S. Goindi and P. Sarkar, "Dry machining: A step towards sustainable machining - Challenges and future directions," *Journal of Cleaner Production*, vol. 165, pp. 1557–1571, 2017.

[6] X. Wang, B. Zhang, Y. Qiao, and F. Sun, "Chemo-mechanical abrasive flow machining (CM-AFM): a novel high-efficient technique for polishing diamond thin coatings on inner hole surfaces," *Journal of Manufacturing Processes*, vol. 69, pp. 152–164, 2021.

[7] C. S. S. Anupama, L. Natrayan, E. Laxmi Lydia et al., "Deep learning with backtracking search optimization based skin lesion diagnosis model," *Computers, Materials & Continua*, vol. 70, no. 1, pp. 1297–1313, 2022.

[8] F. S. F. Ribeiro, J. C. Lopes, E. C. Bianchi, and L. E. de Angelo Sanchez, "Applications of texturization techniques on cutting tools surfaces—a survey," *International Journal of Advanced Manufacturing Technology*, vol. 109, no. 3–4, pp. 1117–1135, 2020.

[9] N. M. El Basiony, E. E. Badr, S. A. Baker, and A. S. El-Tabei, "Experimental and theoretical (DFT&MC) studies for the adsorption of the synthesized Gemini cationic surfactant based on hydrazide moiety as X-65 steel acid corrosion inhibitor," *Applied Surface Science*, vol. 539, article 148246, 2021.

[10] P. Seták, M. Friák, D. Holec, M. Všianská, and M. Sob, "Strength and brittleness of interfaces in Fe-Al superalloy nanocomposites under multiaxial loading: an Ab initio and atomistic study," *Nanomaterials*, vol. 8, no. 11, p. 873, 2018.

[11] P. Bazan, P. Nosal, A. Wierzbicka-Miernik, and S. Kuciel, "A novel hybrid composites based on biopolyamide 10.10 with basalt/aramid fibers: mechanical and thermal investigation," *Composites Part B: Engineering*, vol. 223, p. 109125, 2021.

[12] R. Shrivastava and K. K. Singh, "Interlaminar fracture toughness characterization of laminated composites: a review," *Polymer Reviews*, vol. 60, no. 3, pp. 542–593, 2020.

[13] F. An, C. Lu, Y. Li et al., "Preparation and characterization of carbon nanotube-hybridized carbon fiber to reinforce epoxy composite," *Materials and Design*, vol. 33, no. 1, pp. 197–202, 2012.

[14] R. Chatzimichail, A. Christogerou, S. Bebelis, and P. Nikolopoulos, "Surface and grain boundary energies as well as surface mass transport in polycrystalline MgO," *Journal of Materials Engineering and Performance*, 2021.

[15] M. M. Shaban, A. M. Eid, R. K. Farag, N. A. Negm, A. A. Fadda, and M. A. Migahed, "Novel trimeric cationic pyrdinium surfactants as bi-functional corrosion inhibitors and antiscalants for API 5L X70 carbon steel against oilfield formation water," *Journal of Molecular Liquids*, vol. 305, article 112817, 2020.

[16] A. Tamtögl, E. Bahn, M. Sacchi et al., "Motion of water monomers reveals a kinetic barrier to ice nucleation on graphene," *Nature Communications*, vol. 12, no. 1, pp. 4–11, 2021.

[17] L. Natrayan and A. Merneedi, "Experimental investigation on wear behaviour of bio-waste reinforced fusion fiber composite laminate under various conditions," *Mater. Today Proc.*, vol. 37, Part 2, pp. 1486–1490, 2021.

[18] A. S. Mitko, D. R. Streltsov, P. V. Dmitryakov, A. A. Nesmelov, A. I. Buzin, and S. N. Chvalun, "Evolution of morphology in the process of growth of island poly(p-xylylene) films obtained by vapor deposition polymerization," *Polymer Science, Series A*, vol. 61, no. 5, pp. 555–564, 2019.

[19] B. von Boehn, C. Penschke, X. Li et al., "Reaction dynamics of metal/oxide catalysts: methanol oxidation at vanadium oxide films on Rh(1 1 1) from UHV to 10^{-2} mbar," *Journal of Catalysis*, vol. 385, pp. 255–264, 2020.

[20] M. Yang, Y. Liu, T. Fan, and D. Zhang, "Metal-graphene interfaces in epitaxial and bulk systems: a review," *Progress in Materials Science*, vol. 110, article 100652, 2020.

[21] P. Karapappas, A. Vavouliotis, P. Tsotra, V. Kostopoulos, and A. Paipetis, "Enhanced fracture properties of carbon reinforced composites by the addition of multi-wall carbon nanotubes," *Journal of Composite Materials*, vol. 43, no. 9, pp. 977–985, 2009.

[22] S. L. K. Konuru, V. Umasankar, B. Sarkar, and A. Sarma, "Microstructure and mechanical properties of tungsten and tungsten-tantalum thin film deposited RAFM steel," *Materials Research Innovations*, vol. 24, no. 2, pp. 97–103, 2020.

[23] S. Yogeshwaran, L. Natrayan, G. Udhayakumar, G. Godwin, and L. Yuvaraj, "Effect of waste tyre particles reinforcement on mechanical properties of jute and abaca fiber- epoxy hybrid composites with pre-treatment," *Materials Today: Proceedings*, vol. 37, Part 2, pp. 1377–1380, 2021.

[24] A. Salman, D. Catur, I. Made Septayana, and M. Dani Masterawan, "Tensile strength and bending analysis in producing composites by using vacuum resin infusion (VARI) method for high-voltage insulator application," in *2018 2nd International Conference on Applied Electromagnetic Technology (AEMT)*, pp. 39–43, Lombok, Indonesia, 2018.

[25] M. Wang, Z. Wang, X. Gong, and Z. Guo, "The intensification technologies to water electrolysis for hydrogen production - a review," *Renewable and Sustainable Energy Reviews*, vol. 29, pp. 573–588, 2014.

[26] M. B. Ali, R. Saidur, and M. S. Hossain, "A review on emission analysis in cement industries," *Renewable and Sustainable Energy Reviews*, vol. 15, no. 5, pp. 2252–2261, 2011.

[27] K. Aarthi and K. Arunachalam, "Durability studies on fibre reinforced self compacting concrete with sustainable wastes," *Journal of Cleaner Production*, vol. 174, pp. 247–255, 2018.

[28] Z. Yuan, F. Tao, J. Wen, and Y. Tu, "The dependence of microstructural evolution and corrosion resistance of a sandwich multi-layers brazing sheets on the homogenization annealing," *IEEE Access*, vol. 7, pp. 121388–121394, 2019.

[29] C. W. Tan, Z. G. Jiang, L. Q. Li, Y. B. Chen, and X. Y. Chen, "Microstructural evolution and mechanical properties of dissimilar Al-Cu joints produced by friction stir welding," *Materials and Design*, vol. 51, pp. 466–473, 2013.

[30] D. D. Gorhe, K. S. Raja, S. A. Namjoshi, V. Radmilovic, A. Tolly, and D. A. Jones, "Electrochemical methods to detect susceptibility of Ni-Cr-Mo-W alloy 22 to intergranular corrosion," *Metallurgical and Materials Transactions A, Physical Metallurgy and Materials Science*, vol. 36, no. 5, pp. 1153–1167, 2005.

[31] Q. Lin, W. Dong, Z. Wang, and D. Xue, "Research on galling behavior in square cup drawing of high tensile strength steel," in *2010 International Conference on Digital Manufacturing & Automation*, pp. 212–215, Changcha, China, 2010.